*fishes*

MDPI

*Article*

# Comparative Transcriptomics Reveals the microRNA-Mediated Immune Response of Large Yellow Croaker (*Larimichthys crocea*) to *Pseudomonas plecoglossicida* Infection

**Huazhi Chen [1,2,†], Yameng Zhang [1,†], Guangming Shao [1], You Chen [1], Yibo Shen [1], Yinnan Mu [1,*] and Xinhua Chen [1,2,3,*]**

[1] Key Laboratory of Marine Biotechnology of Fujian Province, College of Marine Sciences, Fujian Agriculture and Forestry University, Fuzhou 350002, China
[2] College of Life Sciences, Fujian Agriculture and Forestry University, Fuzhou 350002, China
[3] Southern Marine Science and Engineering Guangdong Laboratory, Zhuhai 519000, China
* Correspondence: muyinnan@163.com (Y.M.); chenxinhua@tio.org.cn (X.C.)
† These authors contributed equally to this work.

**Abstract:** Visceral white nodules disease (VWND), caused by *Pseudomonas plecoglossicida*, is a common disease among cage-farmed large yellow croaker (*Larimichthys crocea*) in China. However, comprehensive investigations of the molecular defensive mechanisms used by *L. crocea* in response to *P. plecoglossicida* infection remain relatively rare. Here, we constructed transcriptomes of the *L. crocea* spleen at 12 h and 24 h after *P. plecoglossicida* challenge. We identified 518 novel miRNAs and 823 known miRNAs in the spleen of *L. crocea*. Between the challenge and control groups, 32 differentially expressed miRNAs (DEmiRNAs), predicted to target 356 genes, and 1152 differentially expressed mRNAs (DEmRNAs) were identified at 12 h post-infection, while 33 DEmiRNAs, predicted to target 278 genes, and 1067 DEmRNAs were identified at 24 h post-infection. Gene ontology (GO) analysis showed that 146 and 126 GO terms were significantly enriched in the target genes at 12 h and 24 h, respectively. Twenty-eight and four immune-associated Kyoto Encyclopedia of Genes and Genomes (KEGG) pathways were significantly enriched in the target genes at 12 h and 24 h, respectively. Three immune-associated pathways were among those most enriched in the target genes: Toll-like receptor signaling, endocytosis, and C-type lectin receptor signaling. Network analysis identified 47 DEmRNA-DEmiRNA pairs. In particular, the immune-related genes *TLR5S* and *PIGR* were targeted by the miRNAs lcr-miR-7132c and dre-miR-183-5p, respectively. Dual-luciferase assays verified that lcr-miR-7132c downregulated *TLR5S*, suggesting that this miRNA may participate in regulating the immune response of *L. crocea* to *P. plecoglossicida* infection through the TLR5S-mediated signaling pathway. Our results help to clarify the miRNA-mediated immune response of *L. crocea* to *P. plecoglossicida* infection.

**Keywords:** large yellow croaker (*Larimichthys crocea*); microRNA; immune response; *Pseudomonas plecoglossicida*



**Citation:** Chen, H.; Zhang, Y.; Shao, G.; Chen, Y.; Shen, Y.; Mu, Y.; Chen, X. Comparative Transcriptomics Reveals the microRNA-Mediated Immune Response of Large Yellow Croaker (*Larimichthys crocea*) to *Pseudomonas plecoglossicida* Infection. *Fishes* **2023**, *8*, 10. https://doi.org/10.3390/fishes8010010

Academic Editor: Alberto Pallavicini

Received: 14 November 2022
Revised: 17 December 2022
Accepted: 21 December 2022
Published: 23 December 2022



## 1. Introduction

MicroRNAs (miRNAs), which are approximately 22 nucleotides (nt), are small non-coding RNAs (ncRNAs) that function as regulators of gene expression [1–3]. In animal cells, miRNA biogenesis starts with the synthesis of primary miRNAs (pri-miRNAs) using RNA polymerase II. Pre-miRNAs are synthesized from pri-miRNAs in the nucleus by the enzyme Drosha. The pre-miRNAs are transported to the cytoplasm and processed by Dicer, each yielding a 22 nt miRNA duplex [4]. Subsequently, one chain of the miRNA hairpin duplex is loaded into an Argonaute family protein to form the core of the miRNA-induced silencing complex, which binds to the 3′-untranslated region (3′-UTR) of the target mRNA to inhibit the translation or initiate the degradation of the target mRNA [4]. An increasing number

of recent studies have indicated that miRNAs are one of the more abundant classes of molecules regulating genes in the immune and stress responses of various organisms [5–8]. For example, human (*Homo sapiens*) miR-206 regulates immune responses to influenza A virus infection by targeting tankyrase 2 [7], while human (*Homo sapiens*) miRNA let-7i downregulates *Toll-like receptor 4* (*TLR4*), inhibiting the production of β-defensin 2 to reduce defenses against *Cryptosporidium parvum* infection [8].

Due to the important regulatory roles played by miRNAs in the host's innate and adaptive immune response, many studies have used high-throughput sequencing to predict and identify miRNAs and their target immunity-related genes in teleost fish. For example, 922 miRNAs related to innate immunity were differentially expressed (235 upregulated and 687 downregulated) in zebrafish (*Danio rerio*) infected with *Salmonella typhimurium* [9]. Similarly, 63 miRNAs were differentially expressed in Atlantic salmon (*Salmo salar*) infected with *Moritella viscosa*, and most of these miRNAs were responsive to other vertebrates and important regulators of host response to bacterial infection [10]. Finally, high-throughput small-RNA sequencing (sRNA-seq) analysis of the gill tissue of *Larimichthys crocea* infected with *Cryptocaryon irritans* identified 122 differentially expressed miRNAs (DEmiRNAs) associated with the Toll-like receptor signaling pathway, RIG-I receptor signaling pathway, phagosome, and Jak-STAT signaling pathway [11]. These results prompted further investigation of miRNA functions and target genes in fish [12–14]. In zebrafish, dre-miR-142a-5p was shown to target the *IL-6 signal transducer* (*il-6st*), enhancing the IL-6 signaling pathway to protect the host against *Staphylococcus epidermidis* infection [12]. Similarly, olive flounder (*Paralichthys olivaceus*) miR-155 was identified as a molecular adjuvant of DNA vaccine enhancing host innate immune responses to viral hemorrhagic septicemia virus (VHSV) infection [13].

Large yellow croaker (*L. crocea*), a perciform species, is an economically important marine fish in China [15]. In recent years, visceral white nodule disease (VWND), caused by *Pseudomonas plecoglossicida*, is one of the most serious bacterial diseases affecting cultured large yellow croakers [16,17]. Previous studies on the interaction between *P. plecoglossicida* and *L. crocea* have mainly focused on the pathogenicity of *P. plecoglossicida* [17,18]. However, comprehensive examinations of the defensive mechanisms used by *L. crocea* in response to *P. plecoglossicida* infection remain relatively rare. Previously, we characterized gene expression profiles in the *L. crocea* spleen before and after *P. plecoglossicida* infection and demonstrated that multiple energy metabolism pathways and innate immune pathways were activated after *P. plecoglossicida* infection [19]. Here, we aimed to expand on this work by exploring the miRNA-mRNA regulatory networks driving the immune response to *P. plecoglossicida*. First, we analyzed miRNA and mRNA transcriptomes to identify the miRNAs and mRNAs that were differentially expressed in the spleen between the control and *L. crocea* challenged with *P. plecoglossicida*. We combined our analyses of expression profiles to construct miRNA-mRNA regulatory networks that potentially participate in the response of *L. crocea* to *P. plecoglossicida* infection. Our results offer novel insights into the regulatory mechanisms underlying the response of *L. crocea* to *P. plecoglossicida* infection.

## 2. Materials and Methods

### *2.1. L. crocea Challenge and Sampling*

Suspensions of *P. plecoglossicida* ($1 \times 10^5$ colony-forming units, CFU/mL) were prepared as previously described [17]. *L. crocea* (body weight 32.62 ± 5.21 g) were purchased from Fufa Aquatic Product Company Ltd. (Ningde, China) and acclimated in one-ton tanks with aerated seawater at 18 °C for 2 weeks. After the acclimation period, the fish were randomly selected and divided into challenge and control groups ($n$ = 30 per group). Each fish in the challenge group was intraperitoneally injected with 200 µL of the *P. plecoglossicida* suspension ($1 \times 10^5$ CFU/mL), while each fish in the control group was intraperitoneally injected with 200 µL sterilized phosphate buffer saline (PBS). At 12 h and 24 h after injection, five fish per group were randomly selected and anesthetized by eugenol and the spleen

tissues were collected. The spleens of the five fish collected from each group at each time point were pooled. Tissues were frozen with liquid nitrogen and stored at −80 °C.

### *2.2. RNA Extraction, Library Construction, and Comparative Transcriptome Sequencing*

To explore the acute molecular effects of *P. plecoglossicida* challenge on *L. crocea*, three replicate sRNA and RNA libraries were constructed for each of the following four groups: *P. plecoglossicida* challenge at 12 h post-injection (PP-12 h), *P. plecoglossicida* challenge at 24 h post-injection (PP-24 h), control at 12 h post-injection (PBS-12 h), and control at 24 h post-injection (PBS-24 h). Total RNA was extracted from the pooled spleens in each replicate group using the Eastep Super Total RNA Extraction Kit (Promega, Wisconsin, WI, USA), following the manufacturer's instructions. The genomic DNA was removed using DNase I (TaKaRa, Beijing, China). Total RNA concentration and integrity were determined using a nanophotometer (NP80; Implen, Germany) and agarose gel electrophoresis, respectively.

To sequence miRNAs, the small RNAs (16–32 nt) in 20 μg of total RNA were enriched and cleaned using denaturing 15% PAGE. The small RNAs were then connected with sequencing adapters (Illumina, USA) and reverse transcribed into cDNA. The cDNAs were amplified over 15 PCR cycles to produce cDNA libraries. The libraries were validated and quantified using an Agilent 2100 Bioanalyzer and a DNA 1000 Nano Chip Kit (Agilent Technologies, USA), respectively. Small RNA sequencing was performed by Shanghai Majorbio Bio-Pharm Biotechnology Co., Ltd. (Shanghai, China) using a Genome Analyzer Iix (Illumina, San Diego, CA, USA). The raw miRNA sequence reads have been submitted to the NCBI SRA database (accession numbers SRR21397128–SRR21397139).

To sequence mRNAs, RNA-seq libraries were constructed from high-quality RNA samples using the TruSeq RNA Sample Prep Kit (Illumina, USA). Double-terminal sequencing was performed using the Illumina HiSeq X sequencing platform (Illumina, San Diego, CA, USA). The raw mRNA sequence reads have been submitted to the NCBI SRA database (accession numbers SRR21389278–SRR21389289).

### *2.3. Identification of DEmRNAs and DEmiRNAs*

To identify DEmiRNAs between the infected and uninfected transcriptomes, the raw miRNA reads were first cleaned, and the clean reads were then mapped to the reference genome of *L. crocea* (Assembly L_crocea_2.0; accession number: PRJNA354443) [20] using Hisat2 [21]. From the successfully mapped reads, we extracted those that were 18–32 nt long. Non-miRNA reads, including ribosomal RNA (rRNA), small nucleolar RNA (snoRNA), and transport RNA (tRNA), were removed. Known miRNAs were annotated using miRbase (http://www.mirbase.org/), and novel miRNA prediction was performed with miRDeep2 [22]. The novel miRNAs predicted in this study were identified by the label "lcr-miR-N" (Table S1). The relative expression level of each miRNA was calculated using the transcript per million (TPM) method [23]. Differential expression analysis was performed by DESeq2 (Version 1.24.0) [24], and DEmiRNAs were defined as those with $|\text{fold-change}| > 1.5$ and $p < 0.05$.

To identify the differentially expressed mRNAs (DEmRNAs) between the infected and uninfected transcriptomes, the raw mRNA reads were first cleaned, and the clean reads were mapped to the *L. crocea* reference genome (Assembly L_crocea_2.0; accession number: PRJNA354443) using Hisat2 [21]. StringTie v1.3.3b [25] was used to assemble the mapped reads into transcripts. The relative expression level of each mRNA was calculated using the TPM method [23]. Differential expression analysis was performed by DESeq2 (Version 1.24.0) [24], and DEmRNAs were defined as those with $|\text{fold-change}| > 1.5$ and $p < 0.05$.

### *2.4. Association Analysis and Construction of the miRNA-mRNA Regulatory Network*

The genes targeted by the DEmiRNAs were predicted using MiRanda [26] and RNAhybrid [27], and the intersection of the results was retained. The predicted DEmiRNA target genes and the DEmRNAs were annotated using the Kyoto Encyclopedia of Genes and Genomes (KEGG; http://www.genome.jp/kegg/) and the Gene Ontology (GO) database

(http://geneontology.org/). GO terms were considered significant when the Fisher-exact *p*-value was <0.05. DEmiRNA-DEmRNA regulatory networks were constructed using Cytoscape [28] on the OmicShare platform (https://www.omicshare.com).

### *2.5. Verification of Novel miRNAs, DEmiRNAs, and DEmRNAs*

Four of the novel miRNAs were validated by sequencing: the corresponding cDNA sequences were reverse-transcribed using stem-loop primers (Table S2), and Sanger sequencing was performed by Sangon (Shanghai, China). We verified the differential expression patterns of the DEmiRNAs and DEmRNAs using real-time quantitative PCR (RT-qPCR). First, total RNA was reverse transcribed into cDNA using a mixture of random primers and oligo(dT)$_{20}$ primers (Vazyme, Nanjing, China). RT-qPCRs were performed on Thermal cycler Q5 (Life Technologies, Los Angeles, CA, USA). Each reaction mixture (20 µL) contained 10 µL of SYBR Green (Vazyme, Nanjing, China), 0.2 µL of each primer, and 100 ng of template DNA. The cycling conditions were as follows: 95 °C for 1 min, followed by 40 cycles of 95 °C for 10 s and 60 °C for 30 s. The primers used for RT-qPCR are listed in Table S2. The *L. crocea β-actin* (XM_027284923.1) was used as an internal reference for DEmRNA expression, while the *L. crocea U6* (XR_003462831.1) was used as an internal reference for DEmiRNA expression. The relative expression levels of the DEmiRNAs and DEmRNAs were calculated using the $2^{-\Delta\Delta Ct}$ method [29]. Three independent experiments were performed, with three replicates of each amplification.

### *2.6. Dual-Luciferase Reporter Analysis*

TLR5 has been shown to play an important role in the response to bacterial pathogens by recognizing the bacterial flagellin protein [30]. Therefore, dual-luciferase reporter assays were performed to verify the predicted targeting of *TLR5S* by the novel DEmiRNAs lcr-miR-N228 and lcr-miR-N229. The mature sequences of lcr-miR-N228 and lcr-miR-N229 were identical (5′-GACUUGGUCAUAGCUCCUCAGU-3′). Blasting of this mature miRNA sequence against miRbase (https://www.mirbase.org/) indicated that this sequence was similar to the sequences of miR-7132a and miR-7132b (Table S3). These miRNAs were thus renamed lcr-miR-7132c, following miRNA naming conventions [31]. Mimics of lcr-miR-7132c (double-stranded RNA oligonucleotides) and negative control oligonucleotides (NC mimics) were synthesized by Tsingke Biotechnology (Beijing, China). The 3′-UTR of *TLR5S* was synthesized and inserted into the pmiR-GLO luciferase reporter vector to construct the TLR5S-3′UTR-WT vector, and a mutant of the *TLR5S* 3′-UTR sequence was synthesized and inserted into the pmiR-GLO luciferase reporter vector to construct the TLR5S-3′UTR-MUT vector by Tsingke Biotechnology (Beijing, China).

Human embryonic kidney 293T (HEK293T) cells were maintained in DMEM medium (Thermo, MA, USA) supplemented with 10% fetal bovine serum (FBS), 100 U/mL penicillin, and 100 µg/mL streptomycin at 37 °C in an atmosphere of 5% $CO_2$. The HEK293T cells ($5 \times 10^4$ cells/well) were inoculated into 24-well plates (BIOFIL, China) incubated overnight and co-transfected with the pmiR-GLO-TLR5S-WT plasmid (250 ng) or the pmiR-GLO-TLR5S-MUT plasmid (250 ng) plus the lcr-miR-7132c mimic (150 nM) or the control oligonucleotides (150 nM) using the GenMute (SignaGen, Qingdao, China) transfection reagent. After 24 h of incubation, the cells were dissolved by passive lysis buffer and harvested, and the luciferase activity of the lysate of each well was measured with the Dual-Luciferase Reporter Assay System (Promega, Wisconsin, WI, USA) using a GloMax luminometer (Promega, Wisconsin, WI, USA). Renilla luciferase activity was used as the internal reference against which to normalize the firefly luciferase activity. All results were obtained from three independent assays, each of which was performed in triplicate.

### *2.7. Statistical Analysis*

The results of the RT-qPCR analyses and dual luciferase reporter assays were analyzed using Prism 8 (GraphPad, San Diego, CA, USA). Significant differences in expression

level or luciferase activity between the control and infected groups were identified using two-tailed Student's *t* tests; *p*-values < 0.05 were considered statistically significant.

## 3. Results

### *3.1. Overview of the sRNA-Seq Data and the DEmiRNAs*

More than 11 million raw reads were generated for each sRNA-seq library, and more than 88.55% of all reads were retained after quality control; the *Q*30 ratios for all samples were greater than 98.75% (Table 1). The mean Pearson correlations among replicates of PBS-12 h, PBS-24 h, PP-12 h, and PP-24 h were 92%, 93%, 93%, and 92%, respectively (Figure S1A), indicating that the sRNA-seq data were high-quality, repeatable, and reliable.

**Table 1.** Summary of the small RNA-seq dataset.

| Sample | Raw Reads | Clean Reads | Mapped Reads | *Q*30 |
|---|---|---|---|---|
| PBS-12 h_1 | 14,873,980 | 13,430,011 (90.29%) | 9,965,946 (74.21%) | 98.86% |
| PBS-12 h_2 | 13,073,333 | 11,835,003 (90.53%) | 9,709,046 (82.04%) | 98.87% |
| PBS-12 h_3 | 15,481,958 | 13,709,443 (88.55%) | 10,968,433 (80.01%) | 98.88% |
| PBS-24 h_1 | 14,564,415 | 13,416,481 (92.12%) | 8,802,529 (65.61%) | 98.79% |
| PBS-24 h_2 | 13,325,699 | 11,955,087 (89.71%) | 9,225,816 (77.17%) | 98.75% |
| PBS-24 h_3 | 13,852,531 | 12,773,001 (92.21%) | 6,039,554 (47.28%) | 98.79% |
| PP-12 h_1 | 16,836,202 | 15,154,185 (90.01%) | 12,840,447 (84.73%) | 98.86% |
| PP-12 h_2 | 11,060,707 | 10,177,970 (92.02%) | 8,270,715 (81.26%) | 98.81% |
| PP-12 h_3 | 12,941,407 | 11,873,131 (91.75%) | 9,411,944 (79.27%) | 98.85% |
| PP-24 h_1 | 15,204,863 | 13,970,932 (91.88%) | 11,610,363 (83.10%) | 98.81% |
| PP-24 h_2 | 15,249,538 | 14,175,941 (92.96%) | 11,748,698 (82.88%) | 98.81% |
| PP-24 h_3 | 12,695,840 | 11,562,477 (91.07%) | 9,415,271 (81.43%) | 98.88% |

After removing other (non-miRNA) classes of small RNAs (e.g., snRNA, snoRNA, rRNA, and tRNA), 47.28–84.73% of the clean reads mapped to the reference genome. In total, 823 known miRNAs and 518 novel miRNAs were predicted across all sample libraries (Table S1). Four novel miRNAs were randomly selected and validated using Sanger sequencing: lcr-miR-7132c, lcr-miR-N319, lcr-miR-N364, and lcr-miR-N508 (Figure 1A). Most of the predicted miRNAs were 18–26 nt, with sequences of 22 nt the most abundant (708 miRNAs, 52.80% of all sequences; Figure 1B), which was consistent with the expected length of Dicer-processed fragments. Notably, there were significant differences in first nucleotide bias among miRNA sequences of different lengths: the first base of 19–23 nt miRNAs was significantly more likely to be U, the first base of 24–26 nt miRNAs was significantly more likely to be A, and the first base of 18 nt miRNAs was significantly more likely to be G (Figure 1C), which is similar to the miRNAs of other species.

At 12 h post-injection, 32 miRNAs were differentially expressed in the spleens of *L. crocea* challenged with *P. plecoglossicida* as compared to the control *L. crocea*; of these, nine DEmiRNAs were upregulated in the challenged group as compared to the control group, and 23 were downregulated (Table S4 and Figure 1D). At 24 h post-injection, 33 DEmiRNAs were identified between the challenge and control groups, of which 14 were upregulated in the challenge group as compared to the control, and 19 were downregulated (Table S5 and Figure 1D). Five miRNAs were differentially expressed at both time points post-injection (Figure 1E): oni-miR-734, oni-miR-194b, dre-miR-459-5p, dre-miR-194a, and dre-miR-192. These shared DEmiRNAs may play vital roles in the regulation of the response of *L. crocea* to *P. plecoglossicida* infection.

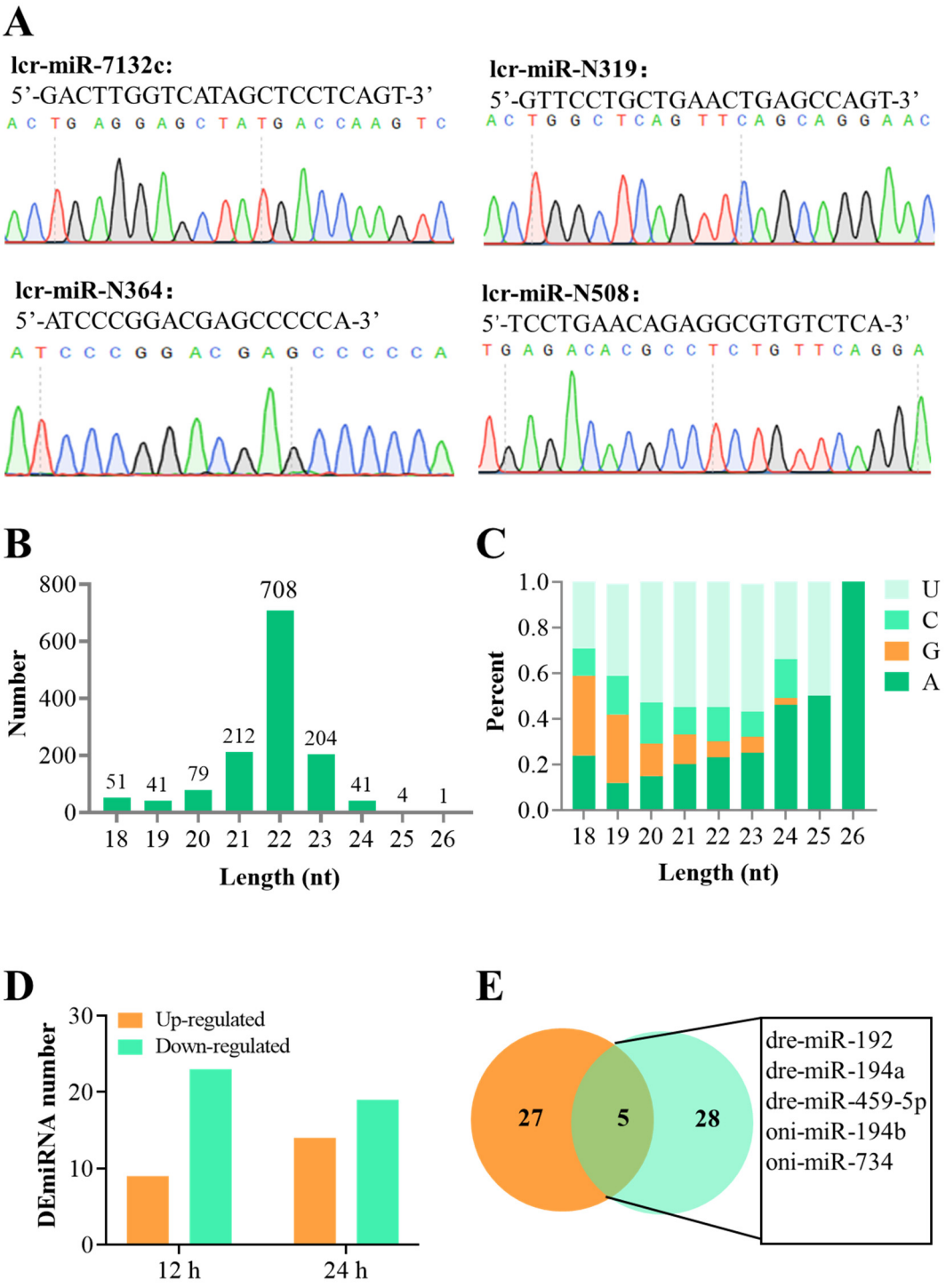


**Figure 1.** Overview of the small RNA-seq data. (**A**) Sanger sequencing validation of the novel miRNAs lcr-miR-7132c, lcr-miR-N319, lcr-miR-N364, and lcr-miR-N508. (**B**) Length distributions of the miRNAs from the *L. crocea* spleen. (**C**) Relationship between first nucleotide bias and miRNA length in the *L. crocea* spleen. (**D**) The number of miRNAs differentially expressed in the spleens of *L. crocea* challenged with *P. plecoglossicida* as compared to the control at 12 h and 24 h after injection. (**E**) Venn diagram showing the unique and shared DEmiRNAs at 12 h (orange) and 24 h (green) after injection.

### *3.2. Overview of RNA-Seq Data and the DEmRNAs*

More than 43 million raw reads were generated for each RNA-seq library, and more than 98.78% of all reads were retained after quality control; the *Q*30 ratios for all samples

were greater than 93.04% (Table 2). The mean Pearson correlations among replicates of PBS-12 h, PBS-24 h, PP-12 h, and PP-24 h were 98.2%, 97%, 97%, and 97%, respectively (Figure S1B), indicating that RNA-seq data were high-quality, repeatable, and reliable.

**Table 2.** Summary of the RNA-seq dataset.

| Sample | Raw Reads | Clean Reads | Mapped Reads | *Q*30 |
|---|---|---|---|---|
| PBS-12 h_1 | 43,759,090 | 43,236,928 (98.81%) | 38,690,266 (89.48%) | 93.22% |
| PBS-12 h_2 | 47,559,984 | 46,977,842 (98.78%) | 41,848,130 (89.08%) | 93.04% |
| PBS-12 h_3 | 46,459,984 | 45,917,460 (98.83%) | 41,084,034 (89.47%) | 93.1% |
| PBS-24 h_1 | 48,368,716 | 47,851,156 (98.83%) | 43,120,810 (90.11%) | 93.49% |
| PBS-24 h_2 | 48,412,476 | 47,868,020 (98.88%) | 42,935,931 (89.7%) | 93.22% |
| PBS-24 h_3 | 50,151,150 | 49,586,402 (98.87%) | 44,435,722 (89.61%) | 93.33% |
| PP-12 h_1 | 47,578,048 | 47,059,414 (98.91%) | 42,137,958 (89.54%) | 93.43% |
| PP-12 h_2 | 45,091,328 | 44,557,844 (98.82%) | 39,893,631 (89.53%) | 93.17% |
| PP-12 h_3 | 50,707,652 | 50,156,332 (98.91%) | 44,954,501 (89.63%) | 93.44% |
| PP-24 h_1 | 46,781,528 | 46,222,554 (98.81%) | 41,453,383 (89.68%) | 93.04% |
| PP-24 h_2 | 46,402,592 | 45,886,162 (98.89%) | 41,196,858 (89.78%) | 93.43% |
| PP-24 h_3 | 52,820,076 | 52,241,174 (98.90%) | 46,817,324 (89.62%) | 93.38% |

Across all samples, 89.08–90.11% of the clean reads were successfully mapped to the reference genome, and 70,294 mRNA transcripts were successfully annotated (Table S6). At 12 h post-injection, 1152 mRNAs were differentially expressed in the spleens of *L. crocea* challenged with *P. plecoglossicida* as compared to the control; of these, 625 DEmRNAs were upregulated in the challenge group as compared to the control group, and 527 were downregulated (Table S7 and Figure 2A). At 24 h post-injection, 1067 DEmRNAs were identified between the control and challenge groups, of which 480 were upregulated in the challenge group as compared to the control and 587 were downregulated (Table S8 and Figure 2A). Venn analysis showed that 74 mRNAs were significantly differentially expressed at both time points post-infection (Figure 2B).

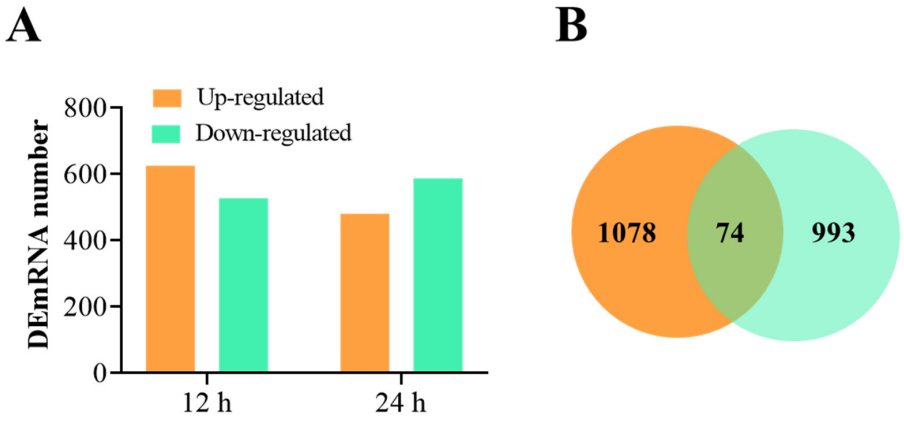


**Figure 2.** Overview of the RNA-seq data. (**A**) The number of mRNAs differentially expressed in the spleens of *L. crocea* challenged with *P. plecoglossicida* as compared to the control at 12 h and 24 h after injection. (**B**) Venn diagram showing the unique and shared DEmRNAs at 12 h (orange) and 24 h (green) after injection.

### *3.3. Prediction and Functional Analysis of DEmiRNA Target Genes*

Prediction analysis suggested that 29 DEmiRNAs targeted 356 genes (736 mRNAs) at 12 h, and that 28 DEmiRNAs targeted 278 genes (557 mRNAs) at 24 h (Tables S9 and S10). GO enrichment analysis suggested that most of the predicted target genes were associated with one of the three GO domains (biological process, molecular function, and cellular component). At 12 h post-injection, the predicted target genes were significantly enriched in 146 GO terms ($p < 0.05$), of which 5 were immune-related: toll-like receptor 5 signaling pathway, regulation

of response to stress, toll signaling pathway, regulation of defense response, and negative regulation of NF-kappa B transcription factor activity (Table S11). At 24 h post-injection, the predicted target genes were significantly enriched in 126 GO terms ($p < 0.05$), of which 3 were immune-related: toll signaling pathway, negative regulation of NF-kappa B transcription factor activity, and activation of MAPK activity (Table S12).

We then explored the biological pathways that potentially participated in the miRNA-driven immune response to *P. plecoglossicida* infection. The genes targeted by DEmiRNAs at 12 h and 24 h post-infection were associated with 74 and 63 KEGG pathways, respectively (Table S13). Two immune-related pathways were among the twenty most enriched KEGG pathways at 12 h post-injection (endocytosis and phagosome; Figure 3A), while three immune-related pathways were among the twenty most enriched KEGG pathways at 24 h post-injection (endocytosis, phagosome, and C-type lectin receptor signaling pathway; Figure 3B).

### *3.4. Functional Analysis of the DEmRNAs*

The mRNAs differentially expressed at 12 h were significantly enriched in 268 GO terms ($p < 0.05$; Table S14); 28 of these terms were immune-related (Table 3). The DEmRNAs at 24 h were enriched in 196 GO terms ($p < 0.05$; Table S15), of which 4 were immune-related (Table 3). At 12 h and 24 h post-infection, 297 and 281 pathways, respectively, were enriched in the DEmRNAs (Table S16). Of these, 29 immune-related pathways were enriched in both sets of DEmRNAs (Figure 4).

**Table 3.** Immunity-related GO terms significantly enriched in the DEmRNAs.

| GO ID | Description | Number of DEmRNAs | *p* Value |
|---|---|---|---|
| GO terms significantly enriched in the DEmRNAs at 12 h post-injection | | | |
| GO:0002274 | Interleukin-8 receptor binding | 3 | 0.000285 |
| GO:0032873 | CXCR chemokine receptor binding | 2 | 0.00031 |
| GO:0060326 | Lysosome | 5 | 0.001027 |
| GO:0005153 | Myeloid leukocyte activation | 2 | 0.001815 |
| GO:0045236 | Negative regulation of stress-activated MAPK cascade | 2 | 0.001815 |
| GO:0042119 | Cell chemotaxis | 2 | 0.001815 |
| GO:0036230 | Neutrophil activation | 2 | 0.001815 |
| GO:0030595 | Granulocyte activation | 4 | 0.003971 |
| GO:0051707 | Leukocyte chemotaxis | 11 | 0.005099 |
| GO:0043207 | Response to other organism | 11 | 0.005564 |
| GO:0009607 | Response to external biotic stimulus | 11 | 0.005727 |
| GO:0043409 | Response to biotic stimulus | 2 | 0.006134 |
| GO:0050900 | Negative regulation of MAPK cascade | 4 | 0.007411 |
| GO:0030593 | Leukocyte migration | 3 | 0.008357 |
| GO:0005764 | Neutrophil chemotaxis | 4 | 0.009344 |
| GO:1990266 | Neutrophil migration | 3 | 0.01046 |
| GO:0071621 | Granulocyte chemotaxis | 3 | 0.011616 |
| GO:0097530 | Granulocyte migration | 3 | 0.01414 |
| GO:0009617 | Response to bacterium | 6 | 0.016991 |
| GO:0002281 | Macrophage activation involved in immune response | 1 | 0.017613 |
| GO:0002366 | Leukocyte activation involved in immune response | 1 | 0.017613 |
| GO:0002263 | Cell activation involved in immune response | 1 | 0.017613 |
| GO:0002275 | Myeloid cell activation involved in immune response | 1 | 0.017613 |
| GO:0071466 | Cellular response to xenobiotic stimulus | 2 | 0.039336 |
| GO:0032526 | Response to retinoic acid | 2 | 0.039336 |
| GO:0045321 | Leukocyte activation | 3 | 0.042277 |
| GO:0031349 | Positive regulation of defense response | 3 | 0.042277 |
| GO:0006952 | Defense response | 9 | 0.046707 |
| GO terms significantly enriched in the DEmRNAs at 24 h post-injection | | | |
| GO:0034138 | Toll-like receptor 3 signaling pathway | 2 | 0.005044 |
| GO:0032642 | Regulation of chemokine production | 2 | 0.005044 |
| GO:0032722 | Positive regulation of chemokine production | 2 | 0.005044 |
| GO:0006909 | Phagocytosis | 2 | 0.047425 |

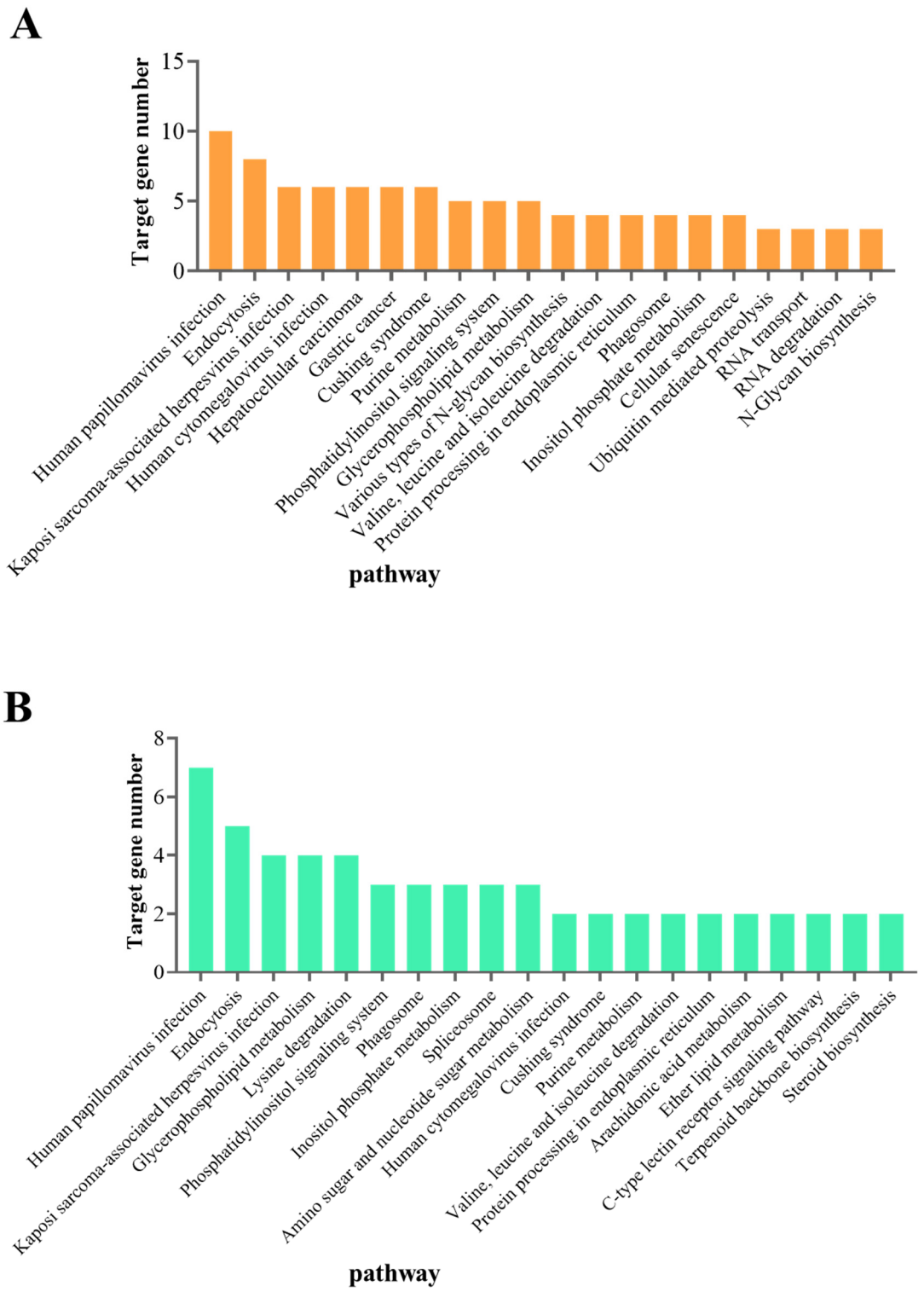


**Figure 3.** The 20 KEGG pathways most enriched in the DEmiRNA target genes at 12 h (**A**) and 24 h (**B**). The x and y axes show the KEGG pathways and the number of associated DEmiRNA target genes, respectively.

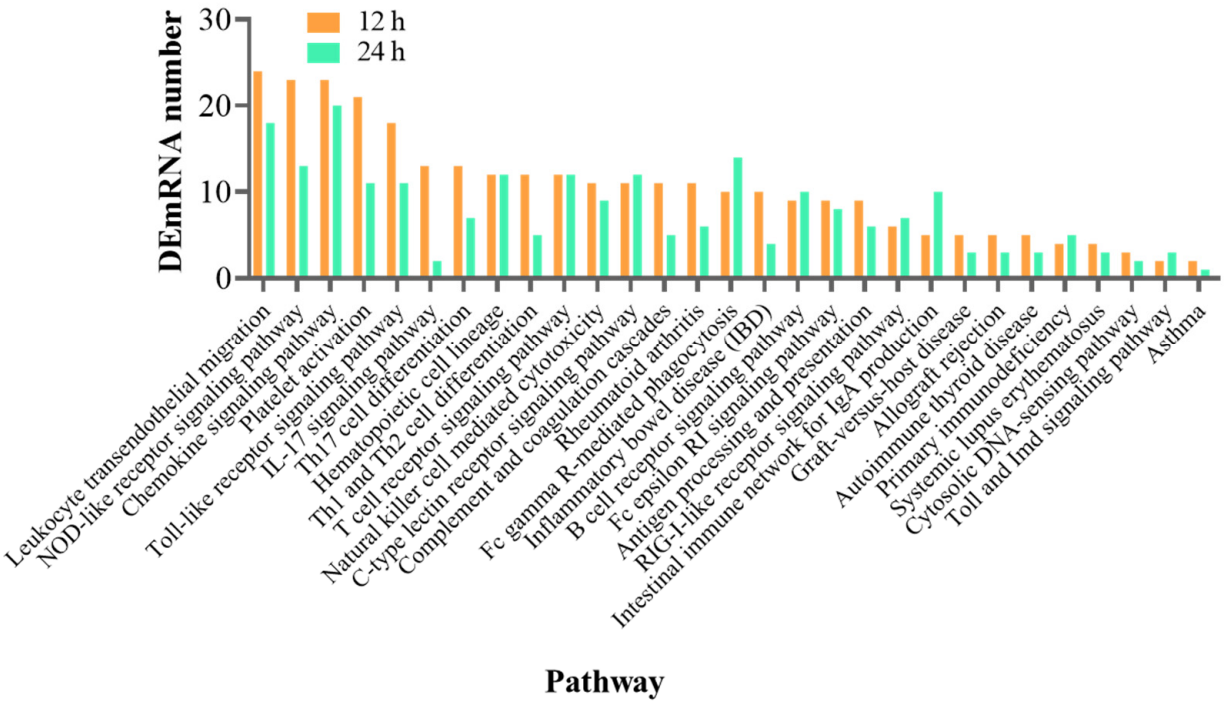


**Figure 4.** Immune-related KEGG pathways enriched in the DEmRNAs. The x and y axes show the KEGG pathways and the number of associated DEmRNAs, respectively.

### *3.5. Integrated Analysis of the DEmiRNA-DEmRNA Regulatory Networks*

Based on the DEmRNAs targeted by the DEmiRNAs, we constructed two DEmiRNA-DEmRNA networks potentially regulating the *L. crocea* response to *P. plecoglossicida* infection in the spleen at 12 h and 24 h (Figure 5). At 12 h, we identified 34 DEmiRNA-DEmRNA pairs, with 12 DEmiRNAs targeting 21 DEmRNAs. Two of these DEmiRNAs, the novel miRNAs lcr-miR-N228 and lcr-miR-N229, targeted the immune-associated gene *TLR5S* (Table S17). The sequences of lcr-miR-N228 and lcr-miR-N229 were identical, and this shared sequence was similar to the sequences of the known miRNAs miR-7132a and miR-7132b. We therefore renamed the two identical miRNAs lcr-miR-7132c. At 24 h, we identified 13 DEmiRNA-DEmRNA pairs, with 8 DEmiRNAs targeting 13 DEmRNAs. Because the DEmiRNA dre-miR-183-5p targeted the immune-related DEmRNA (polymeric immunoglobulin receptor, PIGR), dre-miR-183-5p may play a vital role in regulating PIGR-associated immune pathways (Table S18).

We next aimed to verify the regulatory relationship between lcr-miR-7132c and *TLR5* in vitro. We constructed lcr-miR-7132c mimics, control mimics, reporter plasmids carrying wild-type fragments of the 3′-UTR of *TLR5S*, and reporter plasmids carrying mutated fragments of the 3′-UTR of *TLR5S* (Figure 6A). At 24 h post-transfection, luciferase activity was significantly reduced in cells co-transfected with the wild-type reporter plasmid and the lcr-miR-7132c mimic as compared to those co-transfected with the wild-type reporter plasmid and the non-coding mimics (Figure 6B). However, neither the lcr-miR-7132c mimics nor the non-coding mimics significantly affected luciferase activity in the cells transfected with the mutated reporter plasmid. These results suggested that lcr-miR-7132c might be a negative regulator of *TLR5S* in the spleen of *L. crocea*.

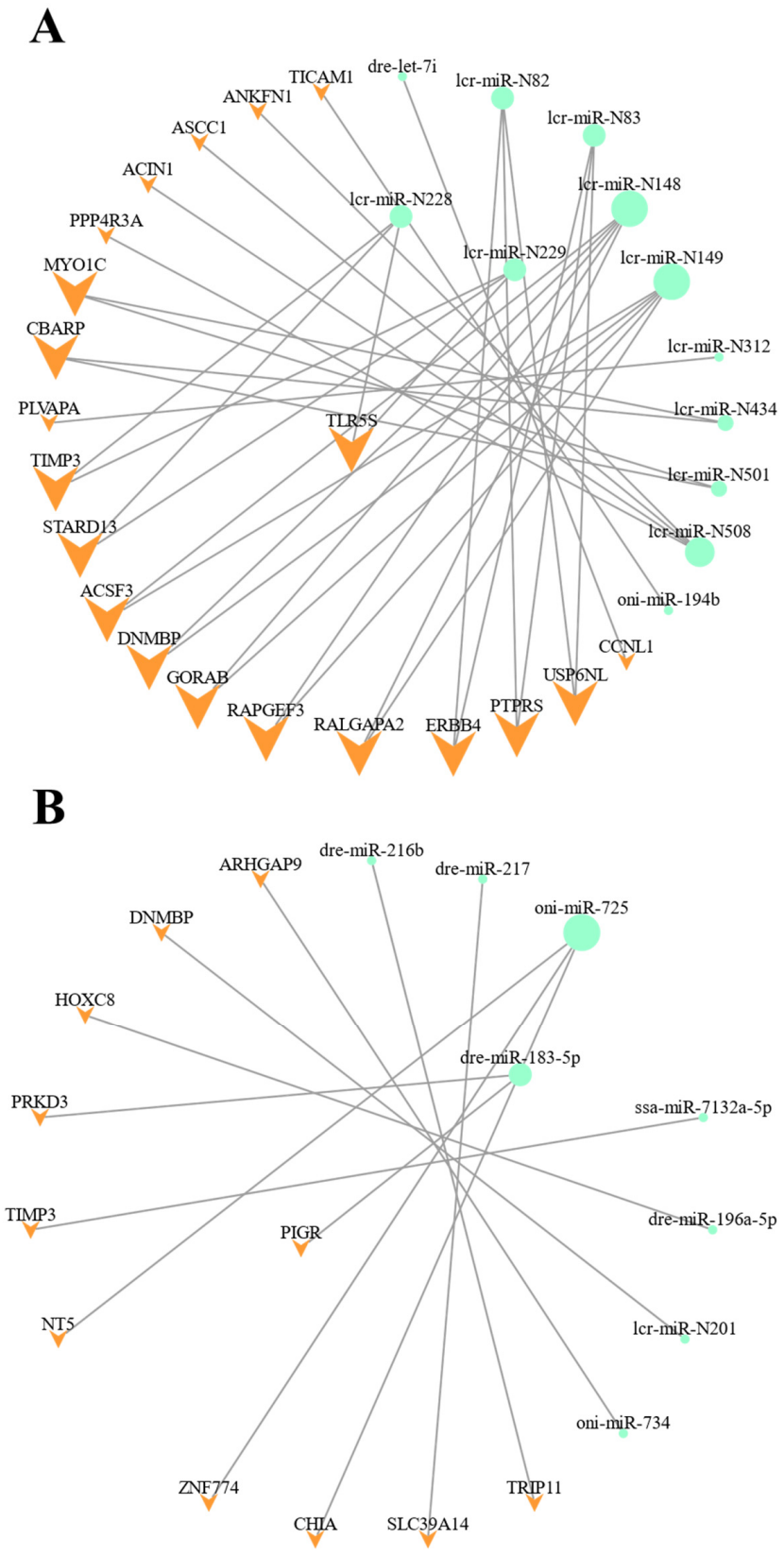


**Figure 5.** The DEmiRNA-DEmRNA regulatory networks identified in spleen of *L. crocea* at 12 h (**A**) and 24 h (**B**) after *P. plecoglossicida* challenge. DEmRNAs are represented by orange arrowheads, and DEmiRNAs are represented by green circles. Shape size reflects the number of associated edges (i.e., larger shapes have a greater number of connections).

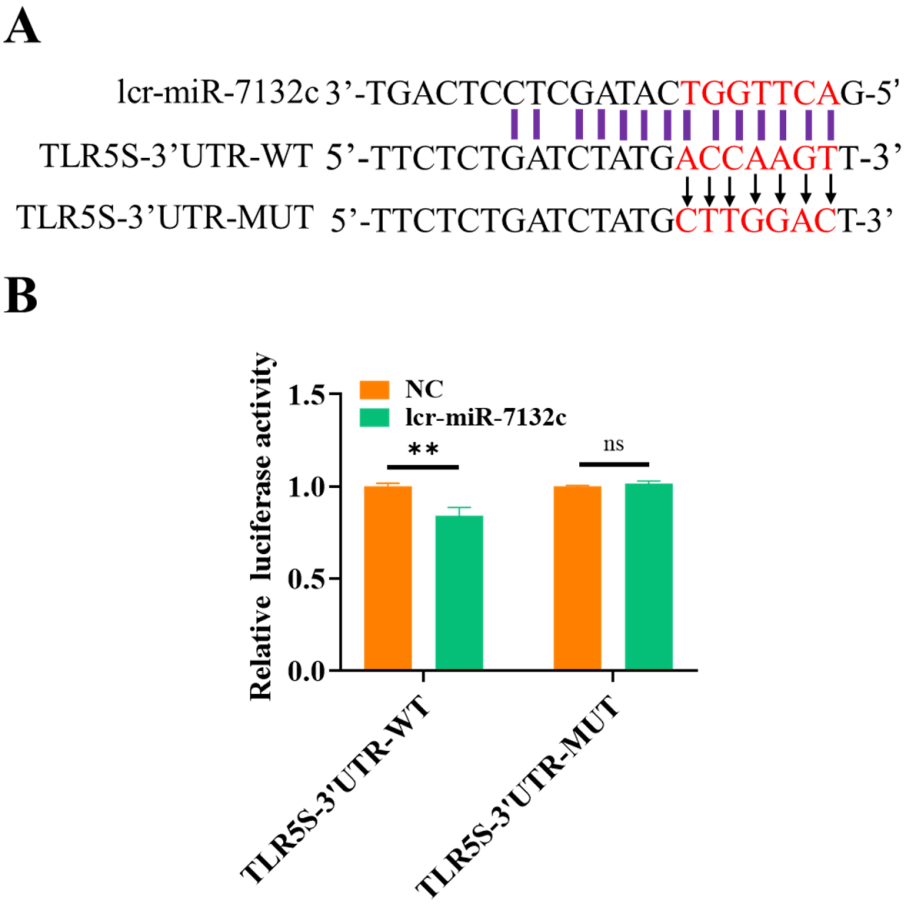


**Figure 6.** In vitro verification of the interaction between DEmiRNA lcr-miR-7132c and DEmRNA *TLR5*. (**A**) Schematic showing the binding between lcr-miR-7132c and the wild-type sequence carried by the control reporter plasmid (TLR5S-3′UTR-WT), as well as the sequence carried by the mutated reporter plasmid (TLR5S-3′UTR-MUT). (**B**) Luciferase activity in HEK293T cells 24 h after co-transfection with TLR5S-3′UTR-WT or TLR5S-3′UTR-MUT and the lcr-miR-7132c mimic or the negative control mimic (NC mimic). Luciferase activity was normalized against Renilla luciferase activity. Error bars represent the SEM of three independent assays. ** $p < 0.01$; ns, not significant.

### *3.6. Validation of the DEmiRNAs and DEmRNAs Using RT-qPCR*

Three DEmRNAs (*B3GNT5A*, *TLR5S*, and *DNMBP*) and three DEmiRNAs (dre-miR-199-3p, lcr-miR-7132c, and lcr-miR-N201) were randomly selected for RT-qPCR validation. The expression patterns were similar across the two types of analyses: *B3GNT5A*, lcr-miR-7132c, and lcr-miR-N201 were downregulated in both the RNA-seq/sRNA-seq data and the RT-qPCR results, while *TLR5S*, *DNMBP*, and dre-miR-199-3p were upregulated in both the RNA-seq/sRNA-seq data and the RT-qPCR results (Figure 7).

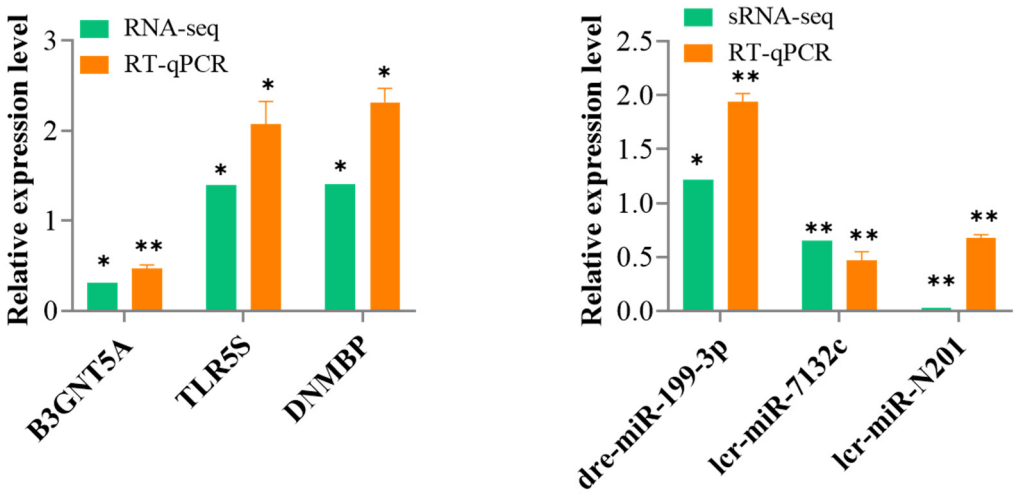


**Figure 7.** Validation of the small RNA- and RNA-seq results. RT-qPCR verification of the differential expression patterns of randomly selected DEmiRNAs and DEmRNAs at 12 h post-injection (*B3GNT5A*, *TLR5S*, dre-miR-199-3p, and lcr-miR-7132c) and at 24 h post-injection (*DNMBP* and lcr-miR-N201). Relative mRNA and miRNA expression levels were calculated with the $2^{-\Delta\Delta Ct}$ method, using *β-actin* and *U6*, respectively, as internal references. Error bars represent the SEM of three independent assays. * $p < 0.05$; ** $p < 0.01$.

## 4. Discussion

The annual production of the large yellow croaker is greater than that of any other cultured marine fish in China [15]. Due to the rapid development of intensive mariculture practices and the consequent deterioration of the average aquaculture environment, diseases have become more frequent in cultured *L. crocea* populations and are now one of the major threats to the *L. crocea* mariculture industry [16]. VWND, which is caused by *P. plecoglossicida*, is one of the most severe diseases affecting cage-farmed *L. crocea* [17]. Antibiotics and chemical drugs remain the preventative treatments for VWND, but extensive use of these measures has led to the accumulation of persistent drug residues, bacterial resistance, and aquatic microecosystem damage [32]. To improve VWND control and reduce the use of environmentally harmful treatments, it is necessary to improve our understanding of the molecular mechanisms underlying the immune response of *L. crocea* to *P. plecoglossicida* infection. The spleen is an important immune organ in teleost fish [33], and previous studies have demonstrated that some miRNAs regulate immune-related genes and pathways in response to bacterial infection in teleost fish [34]. Therefore, we analyzed the differences in the expression patterns of miRNAs and mRNAs in the *L. crocea* spleen in response to *P. plecoglossicida* challenge. Transcriptomic analysis showed that 32 miRNAs and 1152 mRNAs were differentially expressed at 12 h after *P. plecoglossicida* infection, while 33 miRNAs and 1067 mRNAs were differentially expressed at 24 h after *P. plecoglossicida* infection. Of these, 5 miRNAs (8.3%) and 74 mRNAs (3.4%) were differentially expressed relative to control levels at both time points.

Integrated analysis of the DEmiRNA-DEmRNA regulatory networks identified two potential regulatory relationships related to the immune response: dre-miR-183-5p targeting *PIGR* and lcr-miR-7132c (lcr-miR-N228/lcr-miR-N229) targeting *TLR5S*. The PIGR, which is expressed in the immune tissues, binds IgM and IgT to the mucosal tissue as well as binding bacteria, viruses, and parasites [35]. miR-183 has also been implicated in the immune response: this miRNA is aberrantly expressed in autoimmune diseases and plays pleiotropic roles in immunity [36]. For example, miR-183-5p inhibited the *phosphatase and tensin homolog* (*PTEN*) expression to affect the elevation in both phosphorylated AKT and programmed cell death-ligand 1 (PD-L1) expression in human macrophages [37]. Increased miR-183 in lung tumor cells could target the *major histocompatibility complex class I chain-related A/B* (*MICA/B*) to escape detection by natural killer group 2 member D (NKG2D)

receptor on immune cells [38]. In this study, *PIGR*, which was predicted to be targeted by dre-miR-183-5p, was upregulated 24 h after *P. plecoglossicida* infection, and dre-miR-183-5p thus might play a vital role in the immunoglobulin-mediated immune response to *P. plecoglossicida* infection. This result helps to clarify the mechanisms by which fish miRNAs regulate the immune response to bacterial pathogens.

TLRs are vital pattern recognition receptors that recognize highly conserved pathogen-associated molecular patterns (PAMPs) and initiate inflammatory responses against pathogen infection [39]. TLR5 has been shown to recognize the bacterial flagellin protein and to participate in flagellin-mediated NF-κB activation [30]. Two types of TLR5 have been reported in teleosts: the membrane form (TLR5M) and the soluble form (TLR5S) [39–41]. The soluble form, which lacks the Toll/interleukin-1 receptor (TIR) and transmembrane domain, enhances the interaction between flagellin and TLR5M [39–41]. After *P. plecoglossicida* infection, the miRNA lcr-miR-7132c was downregulated and its target gene *TLR5S* was upregulated in the *L. crocea* spleen, suggesting a negative regulatory relationship. This negative regulation of *TLR5S* by lcr-miR-7132c was verified in vitro. Similarly, in miiuy croaker infected with *V. anguillarum*, transcriptomic analysis showed that the downregulation of the miRNAs miR-143-3p and miR-455-3p, which target *TLR5,* was concomitant with the upregulation of *TLR5*, suggesting a negative regulatory relationship [10]. In addition, the overexpression of the miRNAs cid-miRn-115 and miR-142a-3p in grass carp led to the significant downregulation of their target gene *TLR5* [42]. These results suggested that miRNAs may play vital roles in regulating TLR expression and TLR signaling pathways in fish.

## 5. Conclusions

Comparative transcriptome analysis was used to explore the immune-associated response in the spleen of *L. crocea* to *P. plecoglossicida* infection. Analysis of the DEmiRNA-DEmRNA regulatory network identified two miRNA-mRNA pairs related to the immune response: dre-miR-183-5p targeting *PIGR* and lcr-miR-7132c targeting *TLR5S*. The negative regulatory relationship between lcr-miR-7132c and *TLR5S* was verified in vitro using the dual-luciferase reporter system. Our results help to clarify the miRNA-mediated immune response of the teleost host to *P. plecoglossicida* infection.

**Supplementary Materials:** The following supporting information can be downloaded at: https://www.mdpi.com/article/10.3390/fishes8010010/s1, Figure S1: Pearson correlation coefficients of sRNA-seq samples (**A**) and RNA-seq samples (**B**). The color scale represents correlation coefficient; Table S1: Overview of novel miRNAs and known miRNAs; Table S2: Primers used in this study; Table S3: The results of 5′-GACUUGGUCAUAGCUCCUCAGU-3′ in miRbase; Table S4: Information of DEmiRNA at 12 h; Table S5: Information of DEmiRNA at 24 h; Table S6: Overview of mRNA expression in all Samples; Table S7: Overview of DEmRNA at 12 h; Table S8: Overview of DEmRNA at 24 h; Table S9: Overview of DEmiRNA target genes at 12 h; Table S10: Overview of DEmiRNA target genes at 24 h; Table S11: GO enrichment of DEmiRNA target genes at 12 h; Table S12: GO enrichment of DEmiRNA target genes at 24 h; Table S13: KEGG annotation of DEmiRNA target genes at 12 h and 24 h; Table S14: GO enrichment of DEmRNA at 12 h; Table S15: GO enrichment of DEmRNA at 24 h; Table S16: KEGG pathway annotation of DEmRNA at 12 h and 24 h; Table S17: Pairs of DEmiRNA-DEmRNA at 12 h; Table S18: Pairs of DEmiRNA-DEmRNA at 24 h.

**Author Contributions:** Conceptualization, H.C. and Y.Z.; methodology, H.C., Y.Z., Y.C., and Y.S.; software, H.C. and Y.Z.; formal analysis, H.C. and Y.Z.; investigation, H.C. and Y.Z.; resources, H.C., Y.Z., Y.C., and Y.S.; writing—original draft preparation, H.C. and Y.Z.; writing—review and editing, G.S., Y.M., and X.C.; supervision, Y.M. and X.C.; project administration, G.S. and X.C.; funding acquisition, G.S., Y.M., and X.C. All authors have read and agreed to the published version of the manuscript.

**Funding:** This study was supported by grants from the National Key Research and Development Program of China (2018YFD0900602), National Natural Science Foundation of China (U1905204, 32073007, and 32102784), China Agriculture Research System (CARS-47), Innovation Group Project of Southern Marine Science and Engineering Guangdong Laboratory (Zhuhai) (No. 311021006), and Natural Science Foundation of Fujian Province (2022J01211209).

**Institutional Review Board Statement:** The studies were carried out in strict accordance with the Regulations of the Administration of Affairs Concerning Experimental Animals, under protocol license number: SYXK(MIN)2007-0004, approved by the Institutional Animal Care and Use Committee of Fujian Province. All of the surgery was performed under Tricaine-S anesthesia, and all efforts were made to minimize suffering.

**Data Availability Statement:** The raw miRNA sequence reads have been submitted and are available at the NCBI SRA database (accession numbers SRR21397128–SRR21397139). The raw mRNA sequence reads have been submitted and are available at the NCBI SRA database (accession numbers SRR21389278–SRR21389289).

**Acknowledgments:** We thank the referees for their thoughtful comments and recommendations.

**Conflicts of Interest:** The authors declare no conflict of interest. The funders had no role in the design of the study; in the collection, analyses, or interpretation of data; in the writing of the manuscript; or in the decision to publish the results.

## References

1. Komoll, R.M.; Hu, Q.; Olarewaju, O.; von Döhlen, L.; Yuan, Q.; Xie, Y.; Tsay, H.C.; Daon, J.; Qin, R.; Manns, M.P.; et al. MicroRNA-342-3p is a potent tumour suppressor in hepatocellular carcinoma. *J. Hepatol.* **2021**, *74*, 122–134. [CrossRef]
2. Ito, Y.; Matsuzaki, T.; Ayabe, F.; Mokuda, S.; Kurimoto, R.; Matsushima, T.; Tabata, Y.; Inotsume, M.; Tsutsumi, H.; Liu, L.; et al. Both microRNA-455-5p and -3p repress hypoxia-inducible factor-2α expression and coordinately regulate cartilage homeostasis. *Nat. Commun.* **2021**, *12*, 4148. [CrossRef]
3. Kim, E.J.; Kim, J.S.; Lee, S.; Lee, H.; Yoon, J.S.; Hong, J.H.; Chun, S.H.; Sun, S.; Won, H.S.; Hong, S.A.; et al. QKI, A miR-200 target gene, suppresses epithelial-to-mesenchymal transition and tumor growth. *Int. J. Cancer* **2019**, *145*, 1585–1595. [CrossRef]
4. Ha, M.; Kim, V.N. Regulation of microRNA biogenesis. *Nat. Rev. Mol. Cell Biol.* **2014**, *15*, 509–524. [CrossRef]
5. Leung, A.K.; Sharp, P.A. MicroRNA functions in stress responses. *Mol. Cell* **2010**, *40*, 205–215. [CrossRef]
6. Lee, C.Q.E.; Kerouanton, B.; Chothani, S.; Zhang, S.; Chen, Y.; Mantri, C.K.; Hock, D.H.; Lim, R.; Nadkarni, R.; Huynh, V.T.; et al. Coding and non-coding roles of MOCCI (C15ORF48) coordinate to regulate host inflammation and immunity. *Nat. Commun.* **2021**, *12*, 2130. [CrossRef]
7. Bamunuarachchi, G.; Yang, X.; Huang, C.; Liang, Y.; Guo, Y.; Liu, L. MicroRNA-206 inhibits influenza A virus replication by targeting tankyrase 2. *Cell. Microbiol.* **2021**, *23*, e13281. [CrossRef]
8. Chen, X.M.; Splinter, P.L.; O'Hara, S.P.; LaRusso, N.F. A cellular micro-RNA, let-7i, regulates Toll-like receptor 4 expression and contributes to cholangiocyte immune responses against *Cryptosporidium parvum* infection. *J. Biol. Chem.* **2007**, *282*, 28929–28938. [CrossRef]
9. Ordas, A.; Kanwal, Z.; Lindenberg, V.; Rougeot, J.; Mink, M.; Spaink, H.P.; Meijer, A.H. MicroRNA-146 function in the innate immune transcriptome response of zebrafish embryos to *Salmonella typhimurium* infection. *BMC Genom.* **2013**, *14*, 696. [CrossRef]
10. Ramberg, S.; Krasnov, A.; Colquhoun, D.; Wallace, C.; Andreassen, R. Expression analysis of *Moritella viscosa*-challenged Atlantic salmon identifies disease-responding genes, microRNAs and their predicted target genes and pathways. *Int. J. Mol. Sci.* **2022**, *23*, 11200. [CrossRef]
11. Qiao, Y.; Mao, Y.; Wang, J.; Chen, R.; Libing, Z.; Su, Y.Q.; Chen, J.; Zheng, W.Q. Analysis of liver and gill miRNAs of *Larimichthys crocea* against *Cryptocryon irritans* challenge. *Fish Shellfish Immunol.* **2016**, *59*, 484–491. [CrossRef] [PubMed]
12. Dhanagovind, P.T.; Kujur, P.K.; Swain, R.K.; Banerjee, S. IL-6 signaling protects zebrafish larvae during *Staphylococcus epidermidis* infection in a bath immersion model. *J. Immunol.* **2021**, *207*, 2129–2142. [CrossRef] [PubMed]
13. Lim, H.J.; Abdellaoui, N.; Kim, K.H. Effect of miR-155 as a molecular adjuvant of DNA vaccine against VHSV in olive flounder (*Paralichthys olivaceus*). *Fish Shellfish Immunol.* **2019**, *88*, 225–230. [CrossRef] [PubMed]
14. Liyanage, T.D.; Nikapitiya, C.; Lee, J.; De Zoysa, M. Potential immune regulatory role of miR-146a upon *Aeromonas hydrophila* and *Edwardsiella piscicida* infections in zebrafish. *Braz. J. Microbiol.* **2020**, *51*, 931–937. [CrossRef] [PubMed]
15. Peng, J.; Li, W.; Wang, B.; Zhang, S.; Xiao, Y.; Han, F.; Wang, Z. UBE2G1 is a critical component of immune response to the infection of *Pseudomonas plecoglossicida* in large yellow croaker (*Larimichthys crocea*). *Int. J. Mol. Sci.* **2022**, *23*, 8298. [CrossRef] [PubMed]
16. Mu, Y.; Huo, J.; Guan, Y.; Fan, D.; Xiao, X.; Wei, J.; Li, Q.; Mu, P.; Ao, J.; Chen, X. An improved genome assembly for *Larimichthys crocea* reveals hepcidin gene expansion with diversified regulation and function. *Commun. Biol.* **2018**, *1*, 195. [CrossRef]
17. Li, Q.; Chen, Y.; Xu, L.; Yang, Y.; Wen, Q.; Gu, L.; Ao, J.; Chen, X. Identification and bioactivity of a granulocyte colony-stimulating factor a homologue from large yellow croaker (*Larimichthys crocea*). *Fish Shellfish Immunol.* **2020**, *98*, 167–175. [CrossRef]
18. Wang, L.; Sun, Y.; Zhao, L.; Xu, X.; Huang, L.; Qin, Y.; Su, Y.; Zhang, J.; Yan, Q. Dual RNA-seq uncovers the immune response of *Larimichthys crocea* to the secY gene of *Pseudomonas plecoglossicida* from the perspective of host-pathogen interactions. *Fish Shellfish Immunol.* **2019**, *93*, 949–957. [CrossRef]

19. Zhang, Y.; Lu, L.; Li, C.; Shao, G.; Chen, X. Transcriptome analysis revealed multiple immune processes and energy metabolism pathways involved in the defense response of the large yellow croaker *Larimichthys crocea* against *Pseudomonas plecoglossicida*. *Comp. Biochem. Physiol. Part D Genom. Proteom.* **2021**, *40*, 100886. [CrossRef]
20. Ao, J.; Mu, Y.; Xiang, L.X.; Fan, D.; Feng, M.; Zhang, S.; Shi, Q.; Zhu, L.Y.; Li, T.; Ding, Y.; et al. Genome sequencing of the perciform fish *Larimichthys crocea* provides insights into molecular and genetic mechanisms of stress adaptation. *PLoS Genet.* **2015**, *11*, e1005118. [CrossRef]
21. Kim, D.; Paggi, J.M.; Park, C.; Bennett, C.; Salzberg, S.L. Graph-based genome alignment and genotyping with HISAT2 and HISAT-genotype. *Nat. Biotechnol.* **2019**, *37*, 907–915. [CrossRef] [PubMed]
22. Friedländer, M.R.; Mackowiak, S.D.; Li, N.; Chen, W.; Rajewsky, N. miRDeep2 accurately identifies known and hundreds of novel microRNA genes in seven animal clades. *Nucleic Acids Res.* **2012**, *40*, 37–52. [CrossRef] [PubMed]
23. Li, B.; Dewey, C.N. RSEM: Accurate transcript quantification from RNA-Seq data with or without a reference genome. *BMC Bioinform.* **2011**, *12*, 323. [CrossRef] [PubMed]
24. Love, M.I.; Huber, W.; Anders, S. Moderated estimation of fold change and dispersion for RNA-seq data with DESeq2. *Genome Biol.* **2014**, *15*, 550. [CrossRef] [PubMed]
25. Pertea, M.; Pertea, G.M.; Antonescu, C.M.; Chang, T.C.; Mendell, J.T.; Salzberg, S.L. StringTie enables improved reconstruction of a transcriptome from RNA-seq reads. *Nat. Biotechnol.* **2015**, *33*, 290–295. [CrossRef]
26. Betel, D.; Koppal, A.; Agius, P.; Sander, C.; Leslie, C. Comprehensive modeling of microRNA targets predicts functional non-conserved and non-canonical sites. *Genome Biol.* **2010**, *11*, R90. [CrossRef]
27. Krüger, J.; Rehmsmeier, M. RNAhybrid: microRNA target prediction easy, fast and flexible. *Nucleic Acids Res.* **2006**, *34*, W451–W454. [CrossRef]
28. Shannon, P.; Markiel, A.; Ozier, O.; Baliga, N.S.; Wang, J.T.; Ramage, D.; Amin, N.; Schwikowski, B.; Ideker, T. Cytoscape: A software environment for integrated models of biomolecular interaction networks. *Genome Res.* **2003**, *13*, 2498–2504. [CrossRef]
29. Schmittgen, T.D.; Livak, K.J. Analyzing real-time PCR data by the comparative C(T) method. *Nat. Protoc.* **2008**, *3*, 1101–1108. [CrossRef] [PubMed]
30. Hayashi, F.; Smith, K.D.; Ozinsky, A.; Hawn, T.R.; Yi, E.C.; Goodlett, D.R.; Eng, J.K.; Akira, S.; Underhill, D.M.; Aderem, A. The innate immune response to bacterial flagellin is mediated by Toll-like receptor 5. *Nature* **2001**, *410*, 1099–1103. [CrossRef]
31. Ambros, V.; Bartel, B.; Bartel, D.P.; Burge, C.B.; Carrington, J.C.; Chen, X.; Dreyfuss, G.; Eddy, S.R.; Griffiths-Jones, S.; Marshall, M.; et al. A uniform system for microRNA annotation. *RNA* **2003**, *9*, 277–279. [CrossRef] [PubMed]
32. Yan, L.; Jin, D.; Yang, S.; Li, X.; Li, H.; Hu, S.; Sun, Y.; Yi, G.; Wang, P.; Rang, J.; et al. Pathogenicity of fish pathogen *Pseudomonas plecoglossicida* and preparation of its inactivated vaccine. *Microb. Pathog.* **2022**, *166*, 105488. [CrossRef] [PubMed]
33. Zapata, A.; Diez, B.; Cejalvo, T.; Gutiérrez-de Frías, C.; Cortés, A. Ontogeny of the immune system of fish. *Fish Shellfish Immunol.* **2006**, *20*, 126–136. [CrossRef] [PubMed]
34. Andreassen, R.; Høyheim, B. miRNAs associated with immune response in teleost fish. *Dev. Comp. Immunol.* **2017**, *75*, 77–85. [CrossRef] [PubMed]
35. Salinas, I.; Zhang, Y.A.; Sunyer, J.O. Mucosal immunoglobulins and B cells of teleost fish. *Dev. Comp. Immunol.* **2011**, *35*, 1346–1365. [CrossRef]
36. Ichiyama, K.; Dong, C. The role of miR-183 cluster in immunity. *Cancer Lett.* **2019**, *443*, 108–114. [CrossRef]
37. Luo, C.; Xin, H.; Zhou, Z.; Hu, Z.; Sun, R.; Yao, N.; Sun, Q.; Borjigin, U.; Wu, X.; Fan, J.; et al. Tumor-derived exosomes induce immunosuppressive macrophages to foster intrahepatic cholangiocarcinoma progression. *Hepatology* **2022**, *76*, 982–999. [CrossRef]
38. Trinh, T.L.; Kandell, W.M.; Donatelli, S.S.; Tu, N.; Tejera, M.M.; Gilvary, D.L.; Eksioglu, E.A.; Burnette, A.; Adams, W.A.; Liu, J.; et al. Immune evasion by TGFβ-induced miR-183 repression of MICA/B expression in human lung tumor cells. *Oncoimmunology* **2019**, *8*, e1557372. [CrossRef]
39. Medzhitov, R. Recognition of microorganisms and activation of the immune response. *Nature* **2007**, *449*, 819–826. [CrossRef]
40. Muñoz-Flores, C.; Astuya, A.; Roa, F.J.; Romero, A.; Acosta, J.; Sánchez, O.; Toledo, J.R. Activation of membrane-bound and soluble Toll-like Receptors 5 in *Salmo salar* depends on the MyD88 signalling pathway. *Biochim. Biophys. Acta. Gen. Subj.* **2018**, *1862*, 2215–2225. [CrossRef]
41. Umasuthan, N.; Bathige, S.; Thulasitha, W.S.; Jayasooriya, R.; Shin, Y.; Lee, J. Identification of a gene encoding a membrane-anchored toll-like receptor 5 (TLR5M) in *Oplegnathus fasciatus* that responds to flagellin challenge and activates NF-κB. *Fish Shellfish Immunol.* **2017**, *62*, 276–290. [CrossRef] [PubMed]
42. Xu, X.Y.; Shen, Y.B.; Fu, J.J.; Yu, H.Y.; Huang, W.J.; Lu, L.Q.; Li, J.L. MicroRNA-induced negative regulation of TLR-5 in grass carp, *Ctenopharyngodon idella*. *Sci. Rep.* **2016**, *6*, 18595. [CrossRef] [PubMed]